Report

Modifying Bragg Grating Interrogation System

and

Studying Corresponding Problems

1998

Abstract

An improved fiber Bragg grating (FBG) interrogation system is described. The system utilises time domain multiplexing (TDM) technique based on using pulsed radio frequency modulation combined with slow wavelength tuning of a distributed Bragg reflector (DBR) laser. The system has a dynamic range of 4000 microstrain and a scan rate of 25 Hz.

An interference of serial connected FBGs in that interrogation system was investigated.

An interrogation method used in the system results in one-side pulse-width modulation (PWM) with random sampling. Distortions of this kind of PWM have been analysed.

1. Introduction

This report contains results of research made by diploma student Vadim Makarov supervised by his scientific leader Prof. II Dag Roar Hjelme.

A Master diploma based on this research was successfully defended at St.-Petersburg State Technical University, Russia in June 1998.

The object of our research is an effective FBG interrogation system. We have in mind a number of applications requiring multiplexing of several FBGs, signal frequencies up to tens of Hz and in some cases static, or DC readings.

As the main part of this work, we have changed the laser in the existing interrogation system [1]. The system described in that reference uses a semiconductor distributed feedback (DFB) laser as the source. The sweep range of this laser is constrained to approximately 0.7 nm, corresponding to a dynamic range of approximately 630 με [1]. This is insufficient for many applications. Therefore, we decided to change the laser to a semiconductor DBR laser. The DBR laser that we have allows 5.2 nm sweep range (1549.0–1554.2 nm). This corresponds to dynamic range of at least 4000 microstrain (με).

The system has been successfully modified. After that, we have studied two particular problems:

1. Interference of serial connected FBGs in our interrogation system has been investigated.
2. Distortions in a one-side PWM with random sampling have been analysed.

2. Modifying Interrogation System

Prior to making changes, we rebuilt and checked the existing interrogation system [1]. Then we have changed the laser. For readers who are familiar with the system, the changes are described.

The DBR laser differs from the DFB laser. Important features of the DBR laser are listed below.

1. It has wavelength range of 1549.0–1554.2 nm. This requires using of FBGs with corresponding Bragg wavelength.

2. The efficiency of high-frequency wavelength modulation of the DBR laser decreases above 100 MHz. The laser is current modulated through the phase section.

3. Scanning of the laser wavelength is computer controlled. Tuning is achieved by simultaneous changing of currents in Bragg and phase sections of the laser. Seven mode jumps occur while changing wavelength over the entire range. Each mode jump is accompanied by a short-time disturbation of the laser wavelength. Settling time to practically negligible level is about 200 μs.

Considering these features, necessary changes into the interrogation system have been made. The changes are listed below.

1. Modulation frequency has been changed from 560 MHz to about 100 MHz.

2. We have chosen the scan rate of 25 Hz. This scan rate allows filtering out artefacts due to mode jumps fairly well (see below).

3. We have changed the bandpass filter after the time demultiplexer to the first order lowpass filter. We have set the cutoff frequency of this filter to 440 Hz that seems optimal for FBGs with 150 pm linewidth and chosen scan rate.

The modified system is shown on figure 1. An optical part of the system is shown on figure 2.

A slow sawtooth modulation of the laser wavelength is used to determine Bragg wavelengths of FBGs. A TDM technique based on pulsed radio frequency modulation of the laser is used to multiplex several FBGs.

The wavelength of the DBR laser was swept across the FBGs at a rate of 25 Hz. The sweep range was 5.2 nm (1549.0–1554.2 nm), corresponding to a dynamic range of at least 4000 με. The output from the laser was coupled into the FBGs through a

2×2 coupler. As a way to separate out reflection signals from FBGs in the receiver, differential time delays, using a fiber delay line, were combined with the pulsing of the RF modulation. The fiber delay line was approximately 50 m, corresponding to the time delay of approximately 500 ns for the FBG2. The laser was pulsed frequency modulated at about 100 MHz. The pulse repetition frequency was 1 MHz, and the pulse width was 200 ns. Thus, each RF modulated pulse received from the fiber network was perturbed by one FBG only. Although only two FBGs were used, the system was designed as four-channel.

After the photoreceiver, the signal was mixed down to baseband and demultiplexed. After the time demultiplexing, the signal from each FBG was lowpass filtered. The cutoff frequency of the filter was 440 Hz. A signal close to the derivative of the FBG response could be obtained. The modulation frequency was tuned to get the derivative-type signal of enough amplitude and certain polarity for each FBG.

In the derivative-type signal, zero crossing occurs exactly at Bragg wavelength of a FBG. The zero-crossing trigger determined the Bragg wavelength of FBG by generating pulses whose width was determined by the zero crossing in the derivative-type signal relative to a reference signal. A PWM signal was obtained. By low-pass filtering the PWM signal, a signal amplitude proportional to the pulse width could be obtained. In this way, the decoding electronics generated analog output signal nearly proportional to the Bragg wavelength of the corresponding FBG.

The only problem with the modified system was the insufficient suppression of the optical feedback to the laser. This problem shows as decreasing an output power of the laser when a part of light is reflected back to the laser. Sequentially, it leads to interference between FBGs when their Bragg wavelengths are so close that wavelength responses of FBGs overlap. This problem was decreased to great extent by loosening an optical connector of the laser to introduce an additional loss of about 6 dB.

The modified system has been tested. The FBG strainer (fig. 3) was used to strain the FBG2 glued onto the plastic strip. The plastic strip together with the FBG2 was deformed by moving its free end. The Bragg wavelength of the FBG2 was measured using our interrogation system. Measured Bragg wavelength vs. deformation of plastic strip plot is shown on fig. 4. Although the curve is essentially linear, we cannot measure linearity of the system using this FBG strainer. Mechanical design of the FBG strainer could introduce some nonlinearity. If we would like to measure linearity of the

system, a free piece of fiber with FBG should be stretched and the setup should be thermoisolated from room temperature fluctuations. Mode jumps of the DBR laser lead to local nonlinearities. These nonlinearities are similar for all mode jumps. For example, one of them is shown in details on fig. 5. A maximum wavelength detection error due to the mode jumps is +10 pm.

We were forced to choose fairly low scan rate. It could impose limitations on the number of possible applications of our system. So we have studied frequency limitations of the sampling method (see part 4) and have considered possible measures for increasing the scan rate. We have found two measures.

1. Using the filter of the order more then first will help depressing the artefacts better.

2. We could modify scanning of the laser and the decoding electronics. The laser would not change its wavelength during the settling time after each mode jump. The decoding electronics would be blocked for this time. As we have estimated, this would allow increasing the scan rate at least up to 300 Hz with good results.

3. Interference of Serial Connected Bragg Gratings

Serial connection of FBGs could be an attractive configuration of the optical scheme. In particular, it would use fewer connection fibers and a less complex coupler. However, serially connected FBGs interfere when their Bragg wavelengths get close enough to let their wavelength responses overlap. We have estimated experimentally how much this interference is in the simplest case.

Two serially connected FBGs were used (fig. 6). If we do not take into account multiple reflections then a response of a given FBG is affected only by FBGs placed before it in the chain. Since the FBG1 was the first FBG in the chain, its response was not affected by any other FBG. The FBG2, being the second in the chain, was affected by the FBG1. This affected both the measured wavelength (fig. 7) and the amplitude of response (fig. 8). The maximum wavelength error was 50 pm. The amplitude of the response became roughly 0.25 of normal when Bragg wavelengths of the FBGs were equal. This had been expected since FBG1 attenuated the signal twice, so transmission ratio was

$$(1 - \text{reflectivity\_of\_FBG1})^2 \approx (1 - 0.5)^2 = 0.25.$$

At that point, signal to noise ratio decreased significantly, much more than by 4 times.

The main reason for the interference in the studied case was that the FBG1 acts as the notch filter, not because of multiple reflections.

The maximum wavelength error could be lowered using two possible measures.

1. Using FBGs with a narrower linewidth. At other equal conditions, the maximum wavelength error is proportional to the FBGs linewidth.

2. Using FBGs with a lower reflectance. Although an effect of decreasing the FBGs reflectance depends on a shape of a reflection characteristic of the FBGs, we could roughly estimate that the maximum wavelength error is proportional to the FBGs reflectance.

However, each of these measures could lead to other problems. Using the FBGs with the narrower linewidth would require the lower scan rate. Using the FBGs with the lower reflectance would lower a signal to noise ratio and raise a problem of parasitic reflections. Producing FBGs with special characteristics could be difficult.

4. Distortions in One-Side Pulse-Width Modulation with Random Sampling

Because the scan frequency of the DBR laser is strictly constrained, we have investigated frequency limitations of the sampling method we used. This method converts the Bragg wavelength into PWM signal. That kind of PWM is known as one-side PWM with random sampling[1] (fig. 9). In this case, the Nuquist theory is not quite applicable because sampling time moments depend on the signal.

We have tried a short literature search on this topic with no results. Although it is certainly described somewhere, we have decided to study this problem with practical approach.

We have chosen to simulate this modulation in MATLAB. Our program allows us to compute spectrum of the asymmetric PWM for different input signals[2]. A correctness of the simulation has been successfully checked experimentally. A check has been performed using the interrogation system, an electronically controlled fiber optic Fabry-Perot etalon instead of a Bragg grating and a SR770 FFT network analyzer.

If we set sinusoidal input signal with certain parameters and look at the spectrum then the effects of the one-side PWM with random sampling become clear (fig. 10). A spectrum around each harmonic of the scan frequency is similar to a spectrum of a phase-modulated signal. As for the phase modulation, if we increase the input signal frequency then these spectra become wider (fig. 11). If we increase the amplitude of the input signal then the effective number of harmonics in the spectra grows, so the spectra become wider, too (fig. 12). When the frequency and/or amplitude of the input signal increases enough, harmonics with significant amplitude could appear everywhere including at the signal frequency and the DC component for a number of the signal frequencies.

---

[1] I am not sure whether this term is correct because I have translated it from Russian (noted by VM).

[2] The MATLAB programs, as well as a Word 97 file of this report, are included on the 3”5 floppy disk. However, they are not an example of a good programming style and therefore should be checked carefully before using as a start point for an another simulation.

It is important that the amplitude and phase of the signal in the spectra still constant while the signal frequency changes. The amplitude of the signal in the spectrum is proportional to the modulation signal amplitude at any modulation frequency. Hence, the harmonics only are responsible for distortions.

We need to choose how to quantify distortions in order to estimate a usable range of the input signal parameters. Let the asymmetric PWM be filtered by a lowpass filter. We have chosen to quantify a distortion level by an amplitude ratio of the largest harmonic passed the filter to the signal after filtering (H/S ratio). Although for a particular application an another figure could suit better, the chosen figure is useful in general case.

Figure 13 shows the H/S ratio with brickwall type lowpass filter with cutoff frequency $F_{cutoff} = 0.5*F_{scan}$. Note that consequent slices of the surface are determined by Bessel functions of the first order because amplitudes of harmonics are described through these functions, as shown on the figure. Figure 14 shows the same plot as the family of curves. In the area of the plot affected by the second harmonic ($F_{signal}/F_{scan} > 0.25$), H/S ratio increases rapidly when the amplitude of the signal increases. Therefore, that area is not usable for most applications. The second harmonic would not affect the passband if we choose the lowpass filter with $F_{cutoff} \leq 0.33*F_{scan}$.

For example, magnitude vs. frequency graph for an 8th-order Butterworth type lowpass filter with $F_{cutoff} = 0.3*F_{scan}$ is shown on figure 15. This filter could easily be implemented using a dedicated IC and could be optimal for most applications. Figure 16 shows the H/S ratio with this filter. Corresponding family of curves is shown on figure 17. After the H/S ratio gets noticeable (say, 1%), it increases very rapidly. For practical purposes we have figured out that input signal frequency should be kept below $0.15*F_{scan}$ for large input signal amplitudes and below $0.3*F_{scan}$ for moderate ones.

It was shown above that the spectra around harmonics of the scan frequency behave the same way as the spectrum of phase-modulated signal. That is still true even if we reject an assumption of sinusoidal input signal that was made above. In other words, each harmonic of the scan frequency is phase-modulated by the input signal. Properties of the phase-modulated signal spectrum allow us to spread the results found above on a general case of non-sinusoidal input signal. However, in that general case they should be considered as an approximation only.

5. Summary

The modified FBG interrogation system has been described. The system has dynamic range, scan rate and multiplexing potential exceeding requirements of most possible applications.

The problems constraining scan rate of FBGs was investigated. Among them, distortions in one-side PWM with random sampling represent a common problem for scanning interrogation systems. This problem was thoroughly analysed.

Interference of serial connected FBGs was investigated. Although using serial connection involve certain compromises, it could be acceptable for some applications.

Recommendations for improvement of the system were worked out.

Acknowledgements

The author gratefully acknowledges his supervisor Dag Roar Hjelme for thorough attention to every detail of our work and, particularly, for patiently listening author's terrible English. The author also thanks Jan Rambech, Kjetil Johannessen, Astrid Dyrseth and Noralf Ryen for constant support.

References

1. Hjelme D. R. et al. Application of Bragg grating sensors in the characterization of scaled marine vehicle models// Applied Optics.– Vol. 36, No. 1.– 1997.– Pp. 328–336.

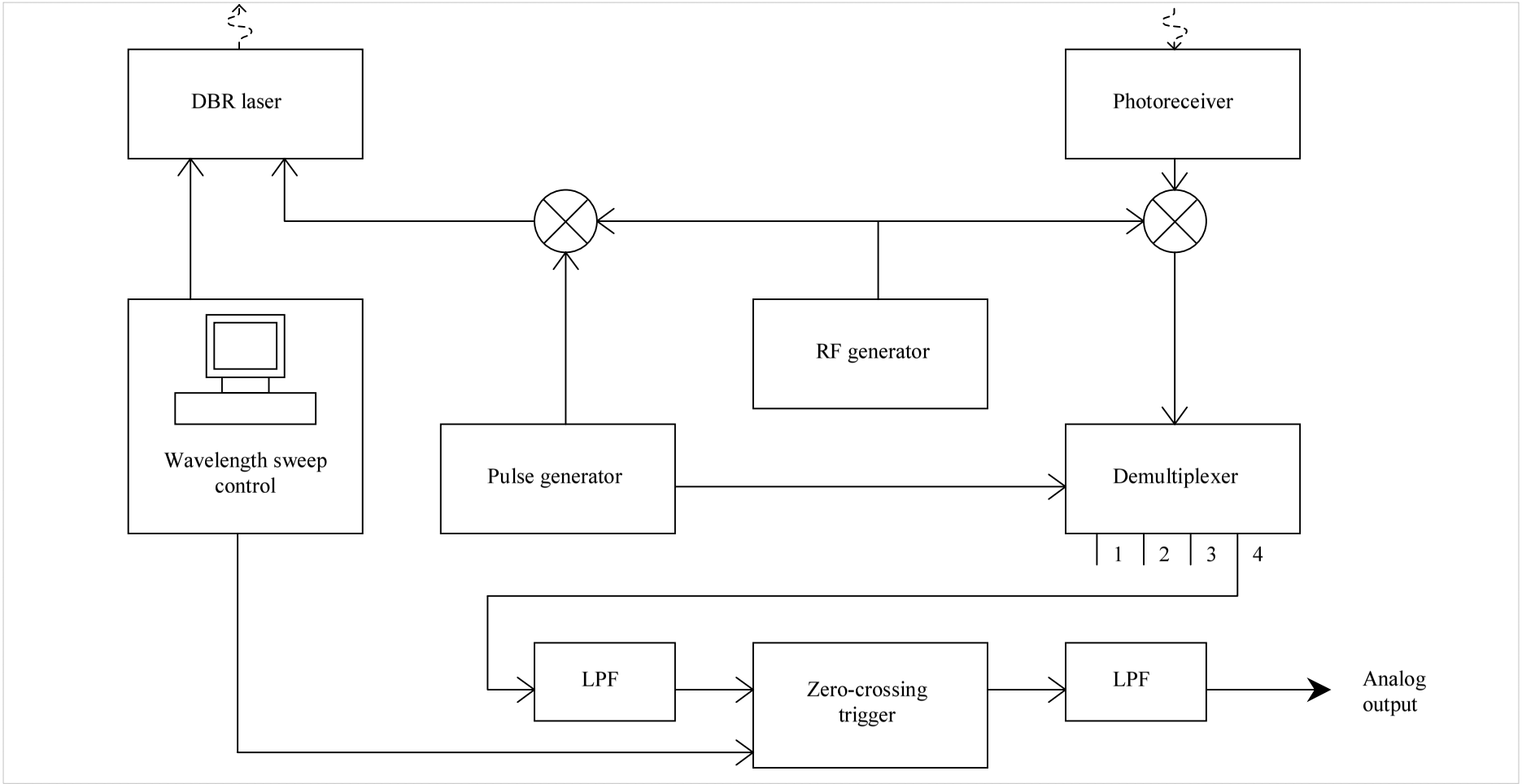

Figure 1. Modified interrogation system

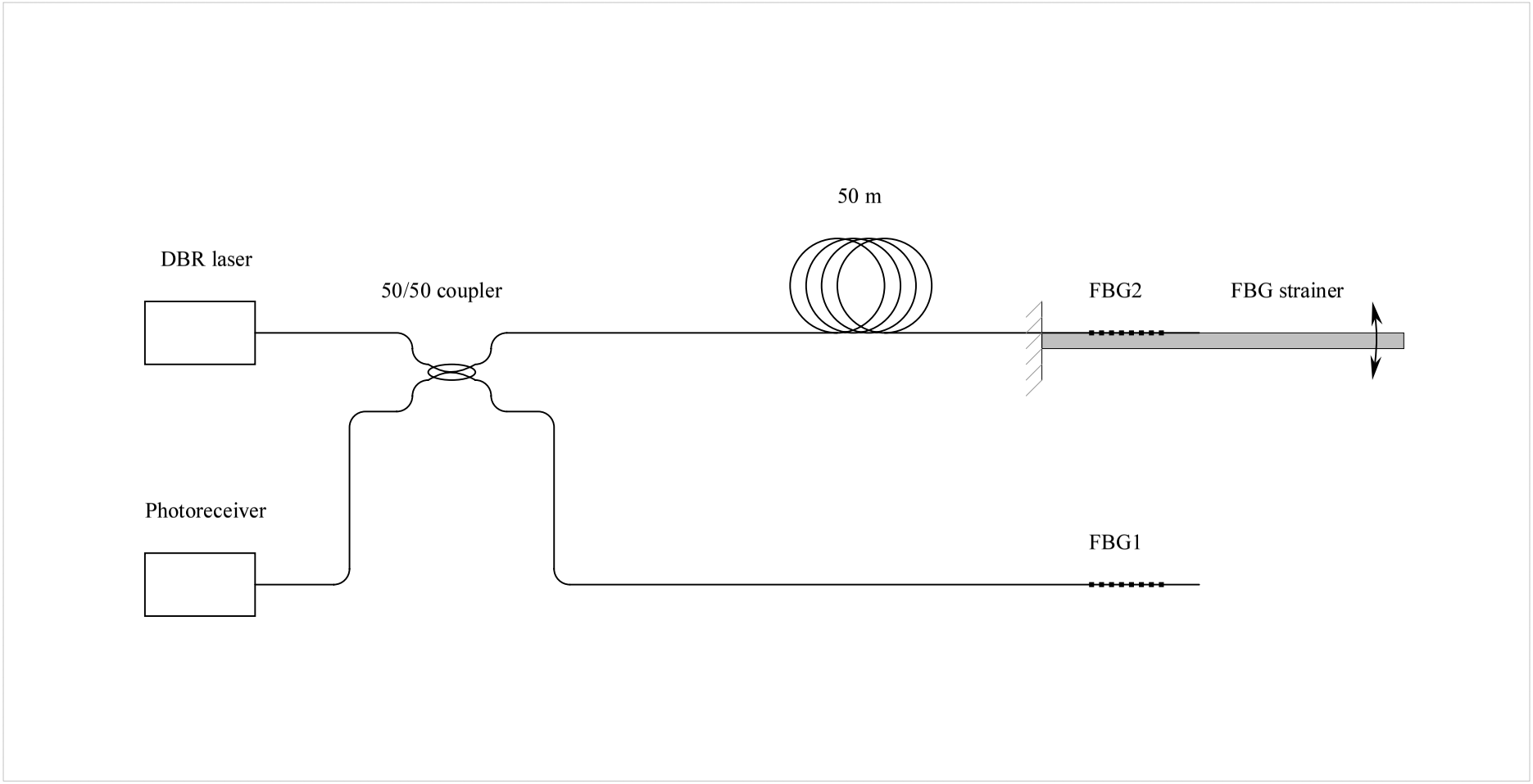

Figure 2. Optical part of the interrogation system we used. There are many connectors not shown. FBG1 and FBG2 made by Innovative Fibers [www.infibers.com], $\lambda \approx 1550.5$ nm, $\Delta\lambda \approx 150$ pm, reflectivity $\approx 50\%$, sidelobs < -30 dB. Department stock numbers of the FBGs were BG 51 and BG 57, correspondingly

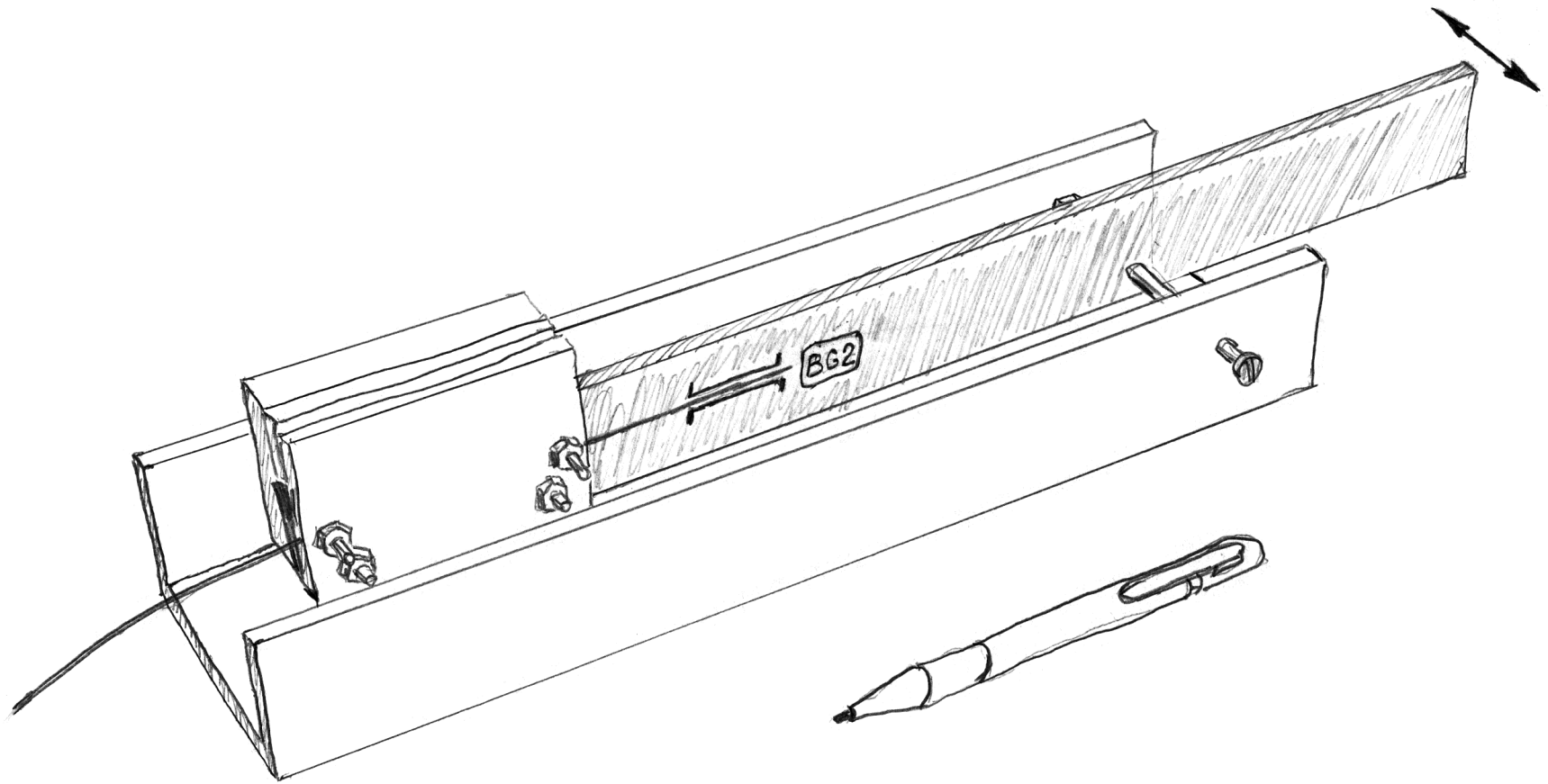

Figure 3. FBG strainer. FBG2 is permanently glued to the plastic strip. The strainer allows changing of its Bragg wavelength by moving the free end of the plastic strip

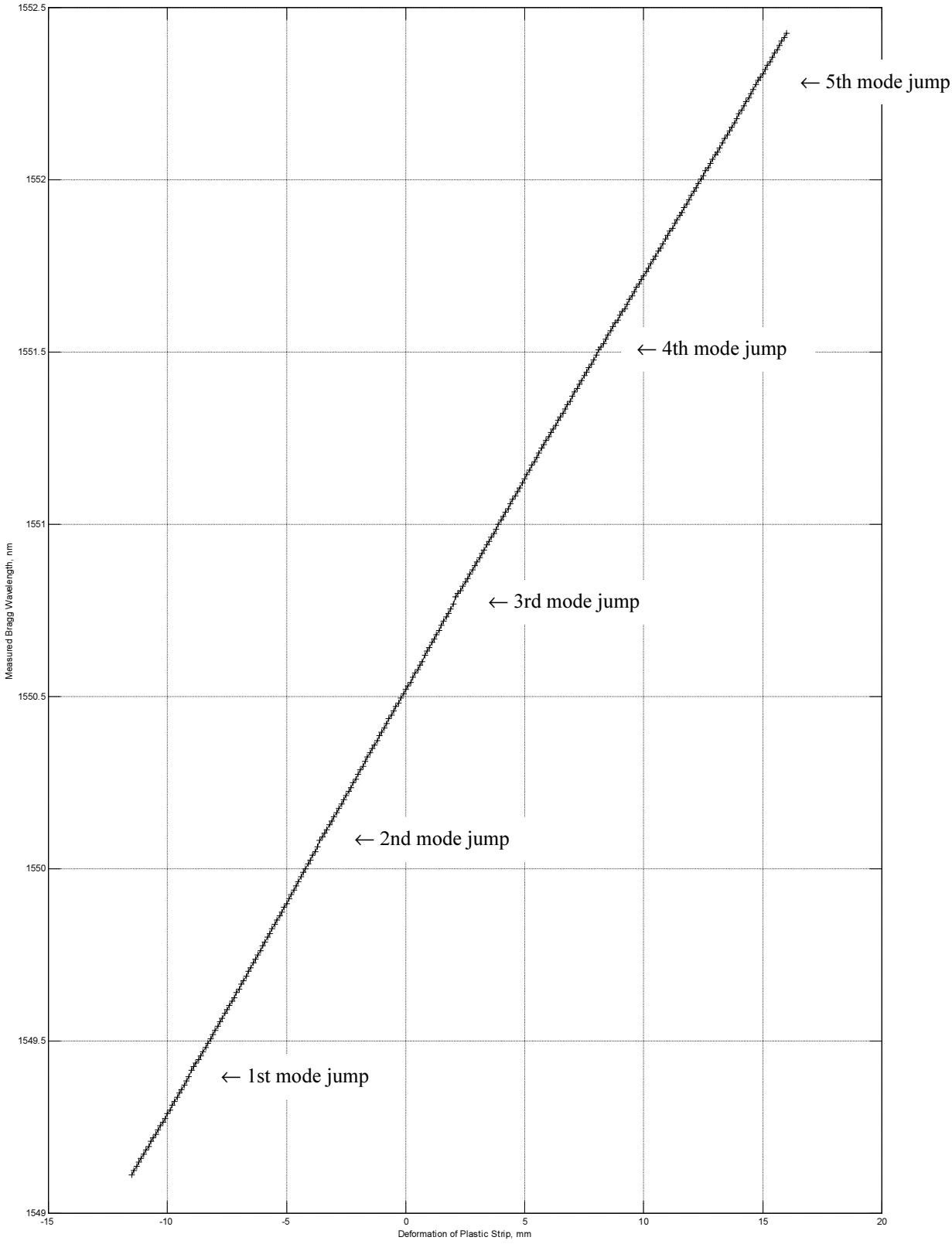

Figure 4. Measured Bragg wavelength vs. deformation of plastic strip

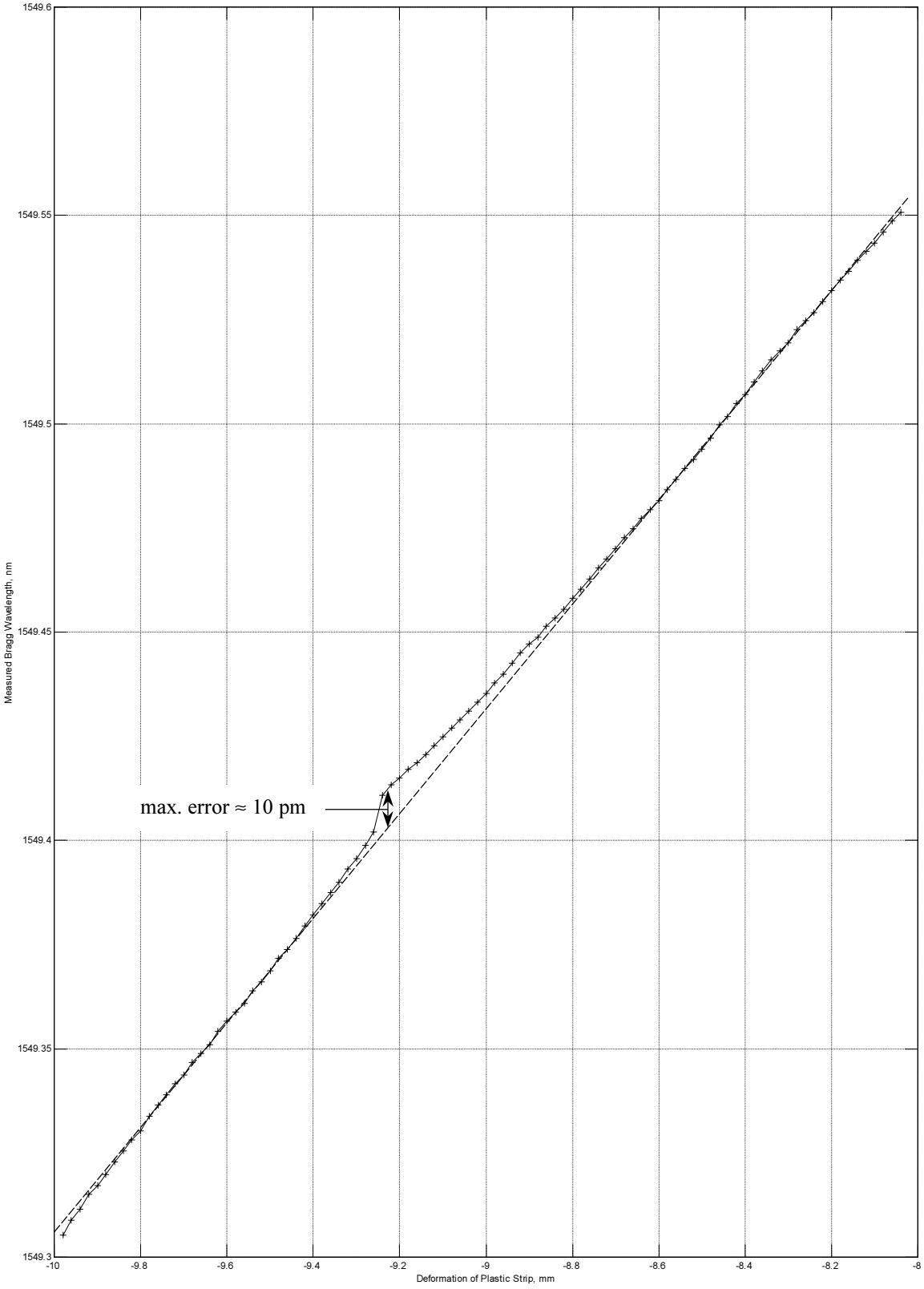

Figure 5. Measured Bragg wavelength vs. deformation of plastic strip. 1st mode jump

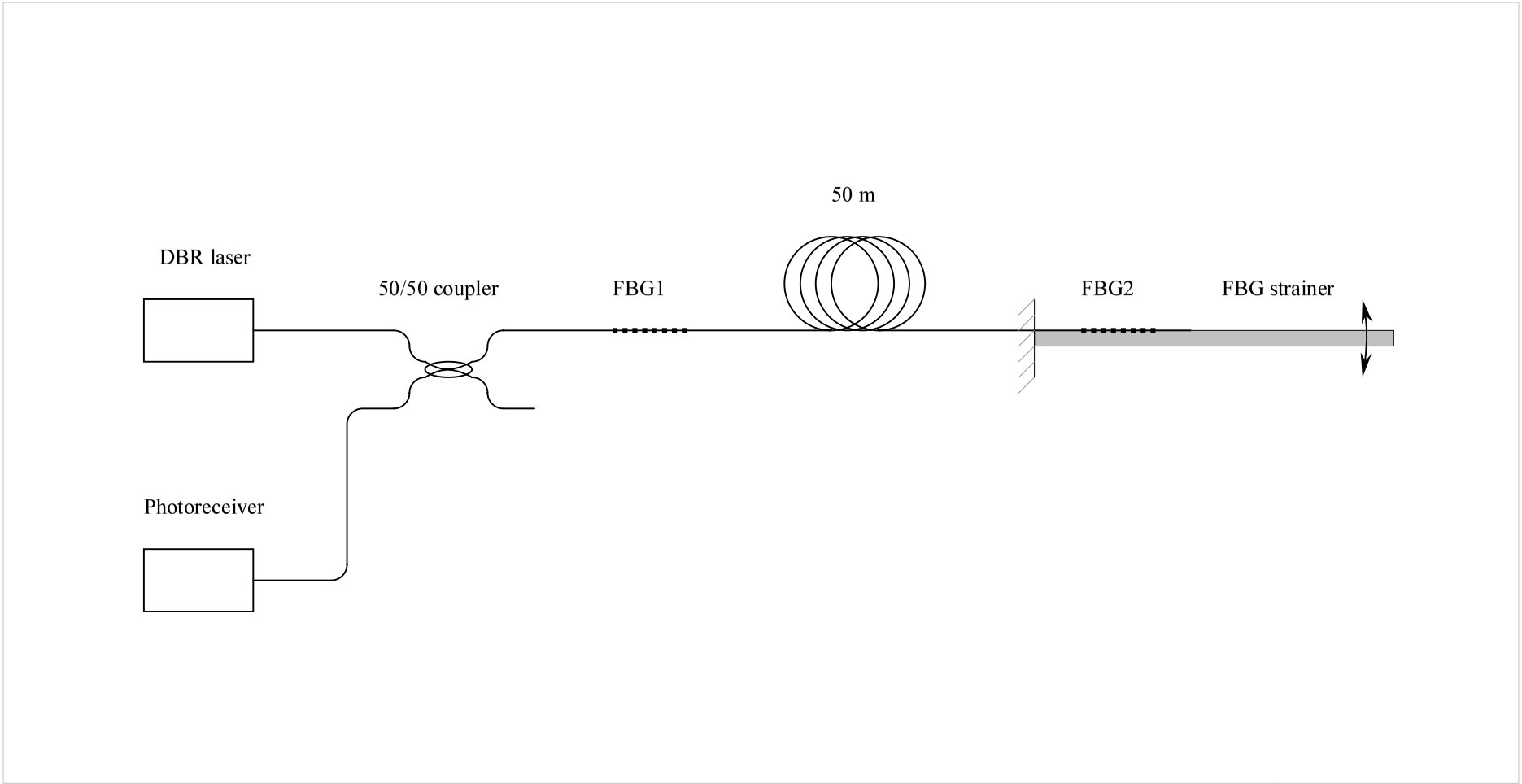

Figure 6. Serial connection of FBGs. The data of FBGs is listed on fig. 2

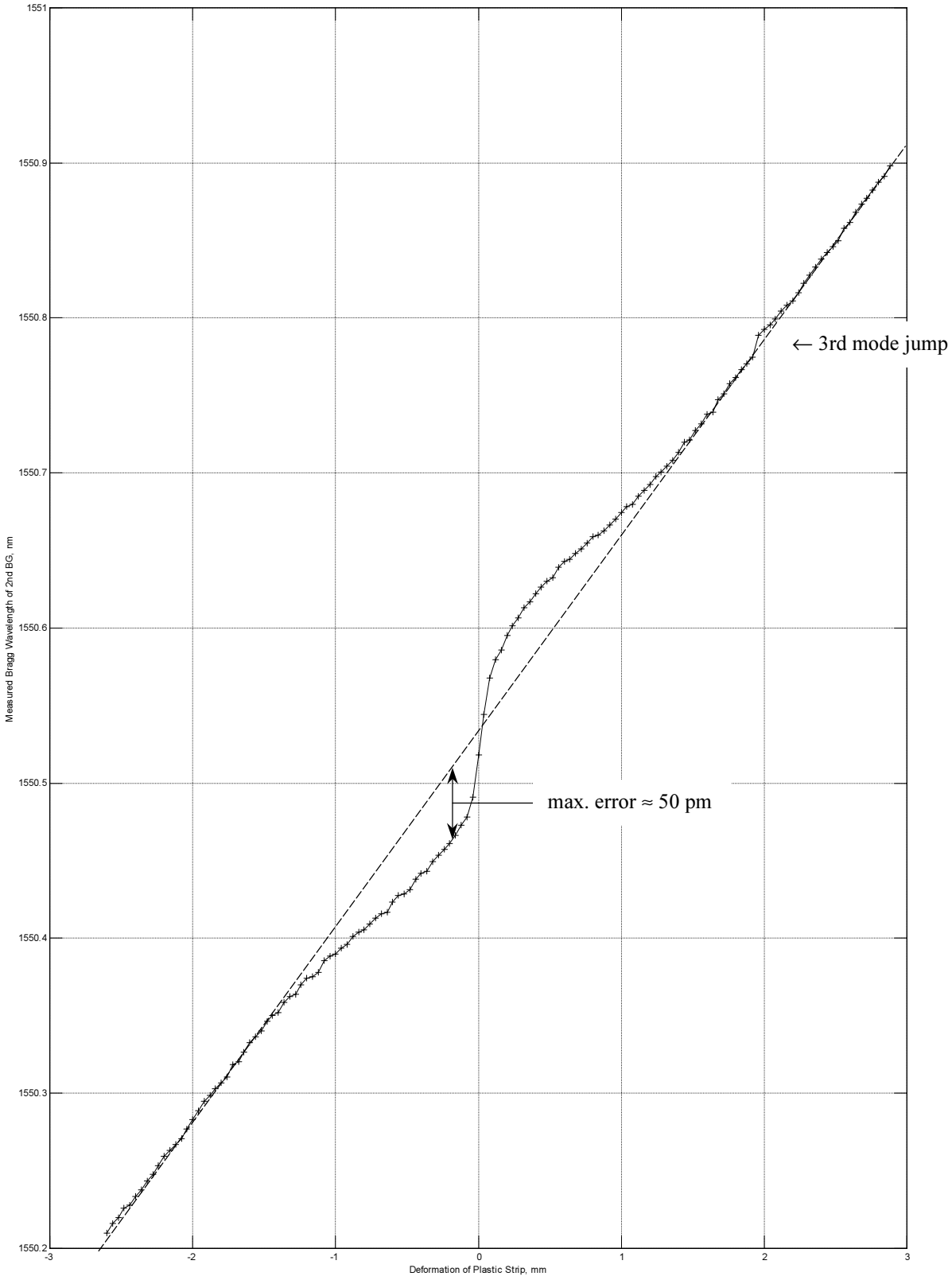

Figure 7. Measured Bragg wavelength of 2nd FBG in serial connection vs. deformation of plastic strip

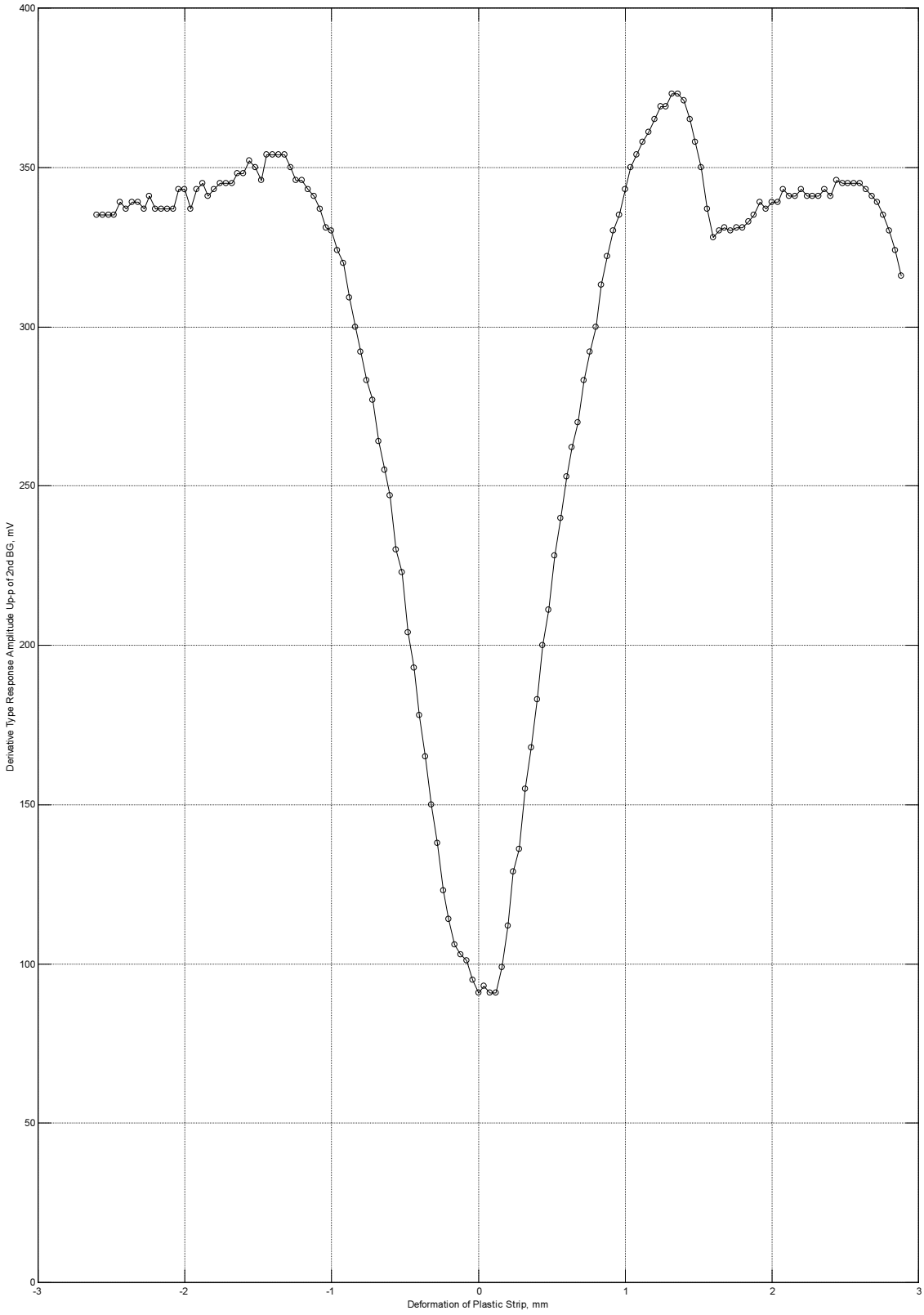

Figure 8. Derivative type response amplitude (p-p) of 2nd FBG in serial connection vs. deformation of plastic strip

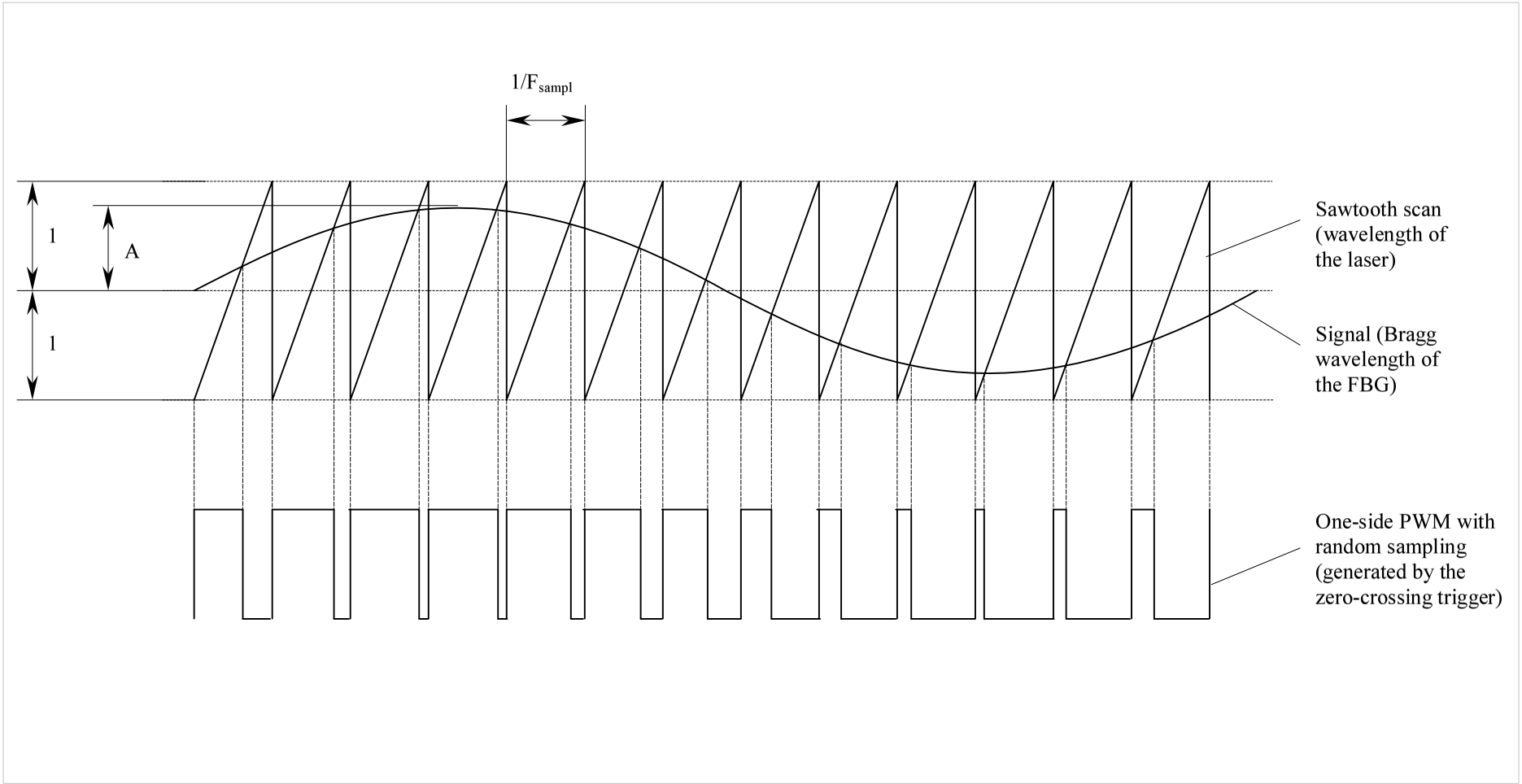

Figure 9. The sampling method we used in the interrogating system results in one-side PWM with random sampling. Changing the DC offset of the signal does not affect our conclusions, so we have centred the signal in the scanning span

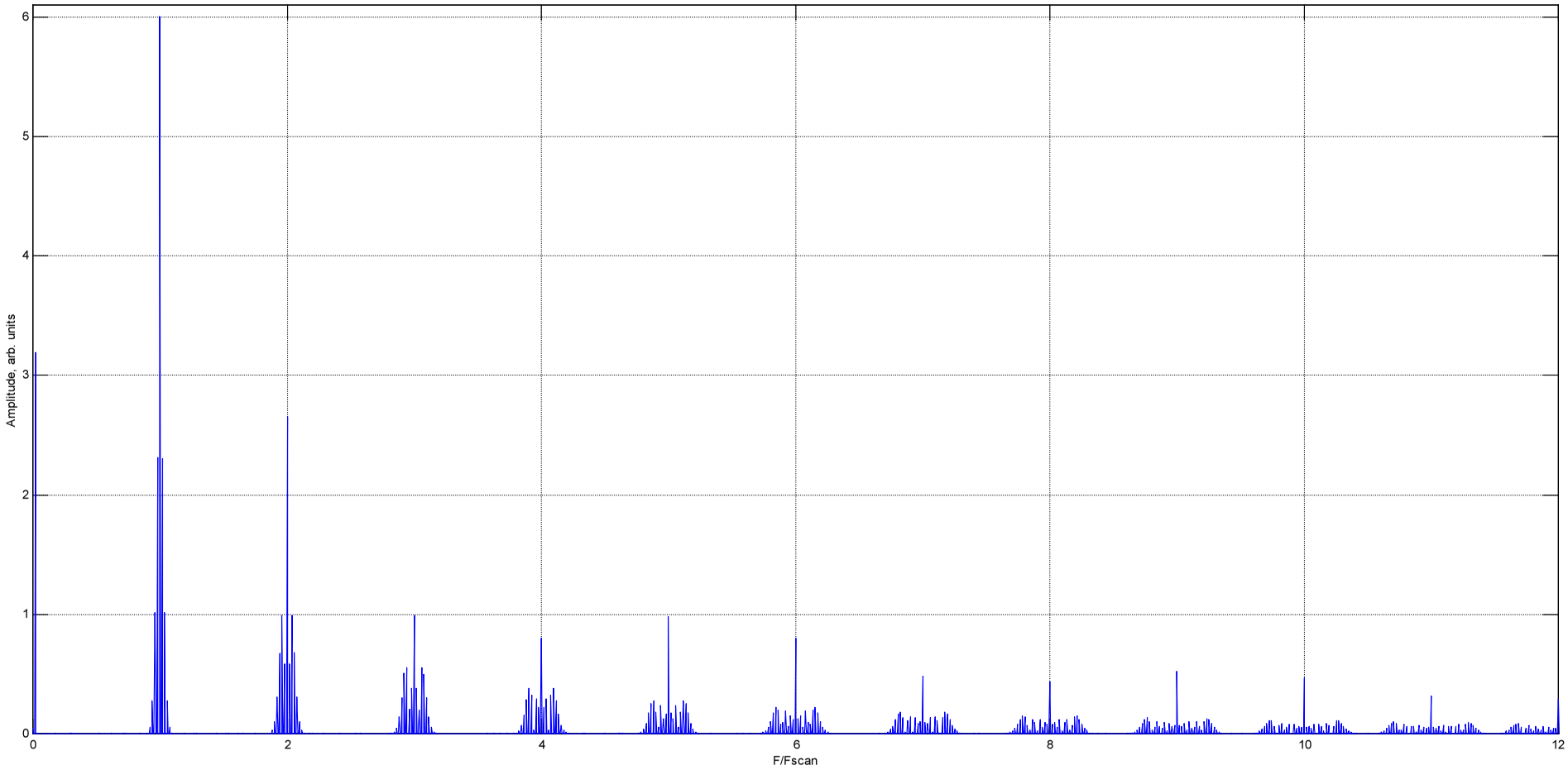

Figure 10. Spectrum of one-side PWM with random sampling. A = 0.5, $F_{signal} = 0.02*F_{scan}$

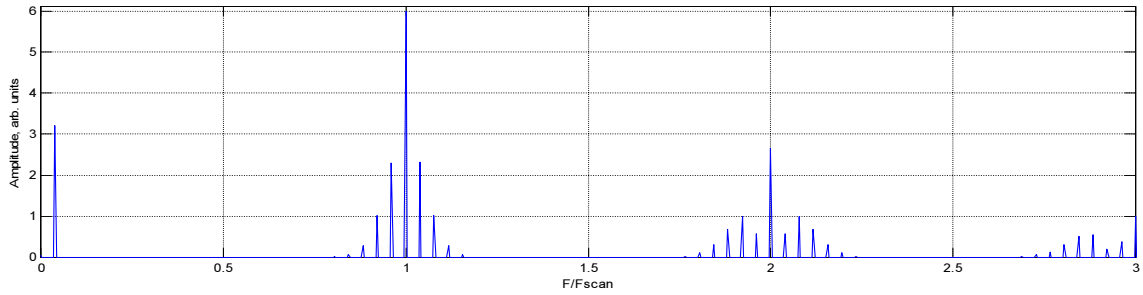

A = 0.5, $F_{signal} = 0.04*F_{scan}$

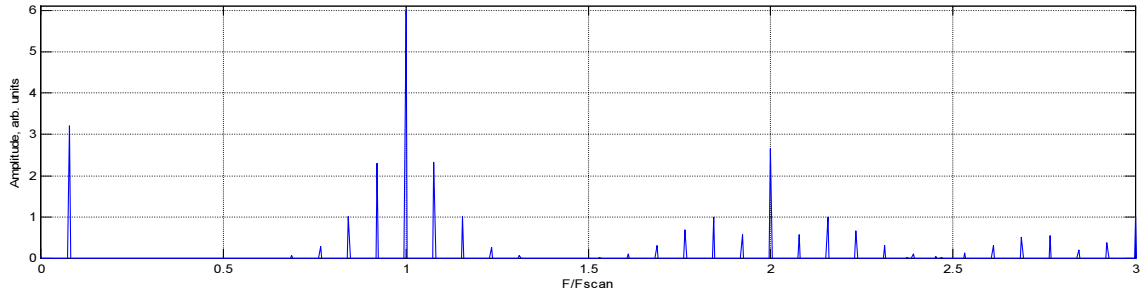

A = 0.5, $F_{signal} = 0.08*F_{scan}$

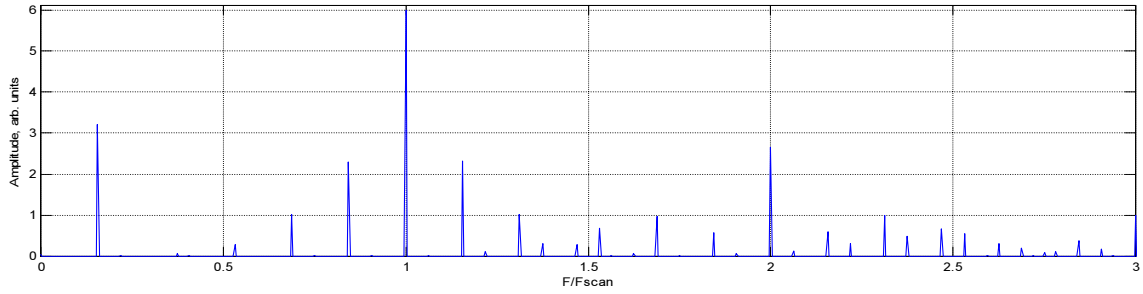

A = 0.5, $F_{signal} = 0.16*F_{scan}$

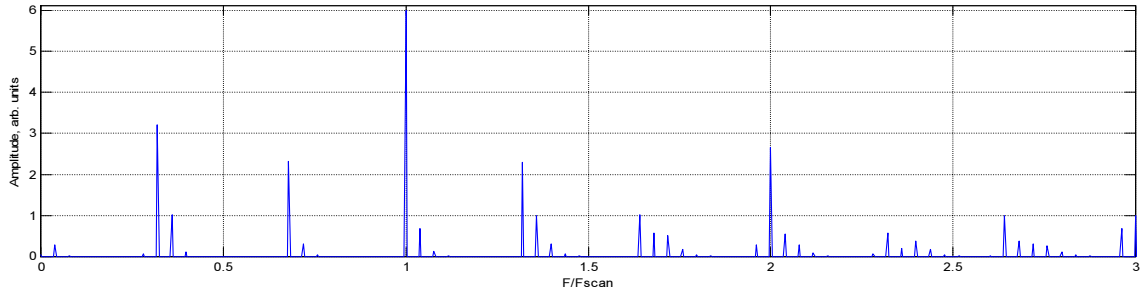

A = 0.5, $F_{signal} = 0.32*F_{scan}$

Figure 11. Spectra of one-side PWM with random sampling for sequentially increasing signal frequency F_{signal}

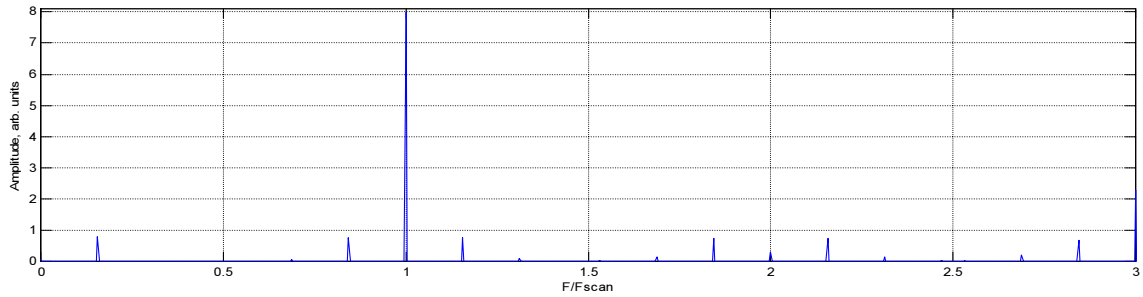

A = 0.125, $F_{signal} = 0.16*F_{scan}$

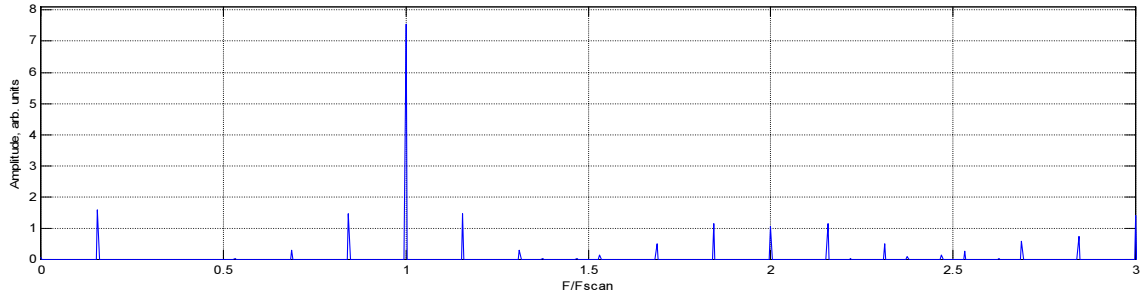

A = 0.25, $F_{signal} = 0.16*F_{scan}$

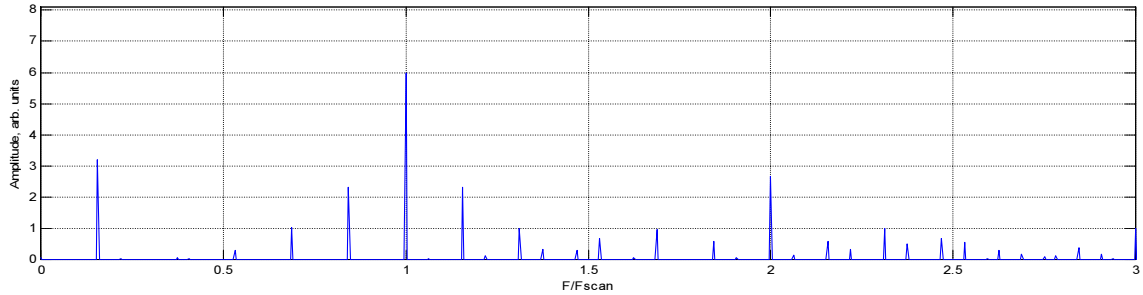

A = 0.5, $F_{signal} = 0.16*F_{scan}$

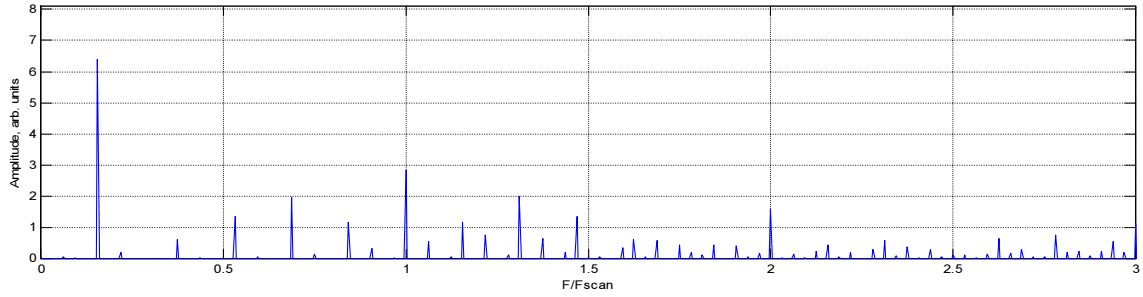

A = 1.0 (max. possible), $F_{signal} = 0.16*F_{scan}$

Figure 12. Spectra of one-side PWM with random sampling for sequentially increasing signal amplitude A

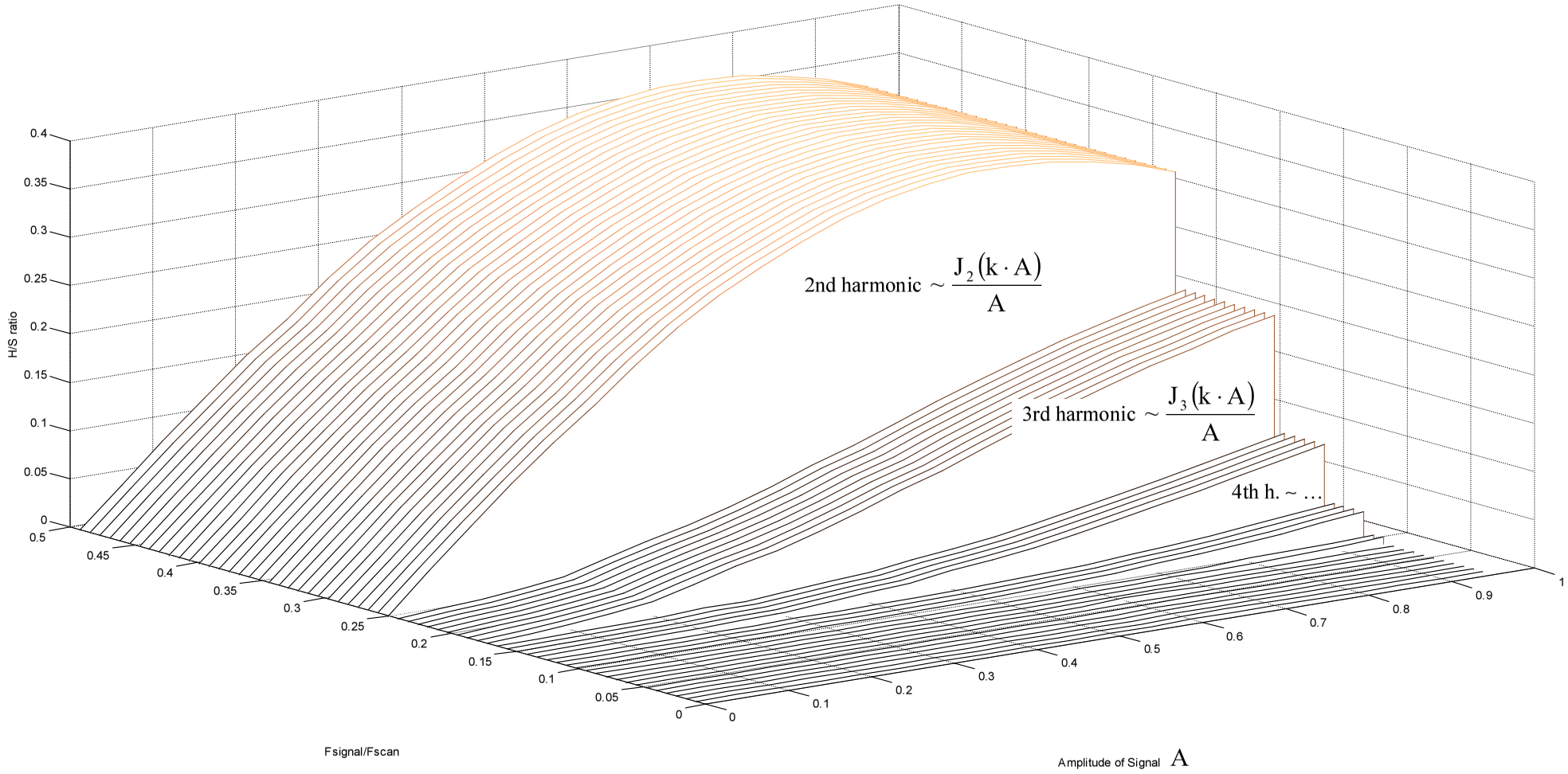

Figure 13. H/S ratio with brickwall type lowpass filter, $F_{cutoff} = 0.5*F_{scan}$

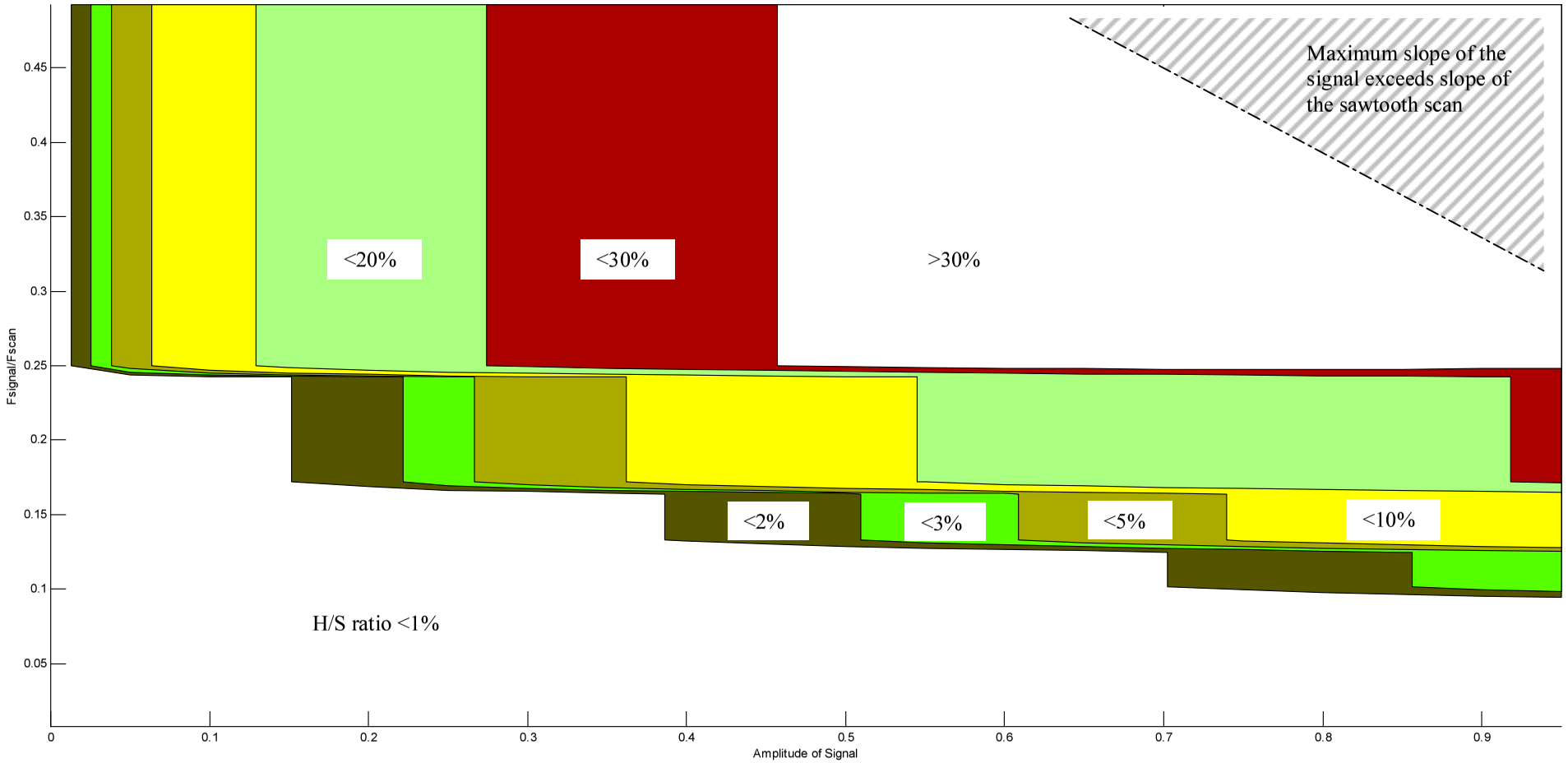

Figure 14. H/S ratio with brickwall type lowpass filter, $F_{cutoff} = 0.5*F_{scan}$

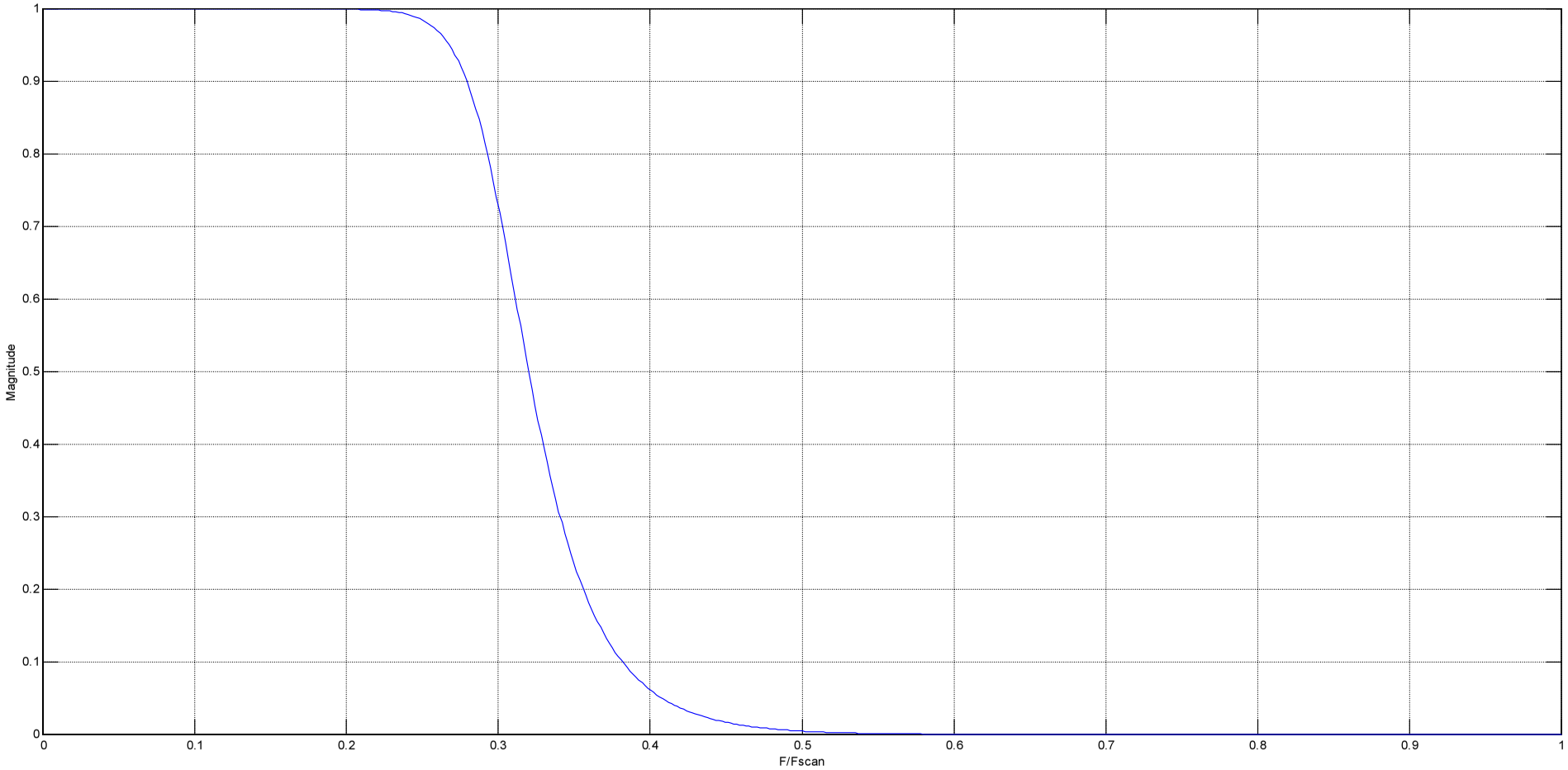

Figure 15. Magnitude vs. frequency graph for 8th-order Butterworth type lowpass filter with $F_{cutoff} = 0.3*F_{scan}$

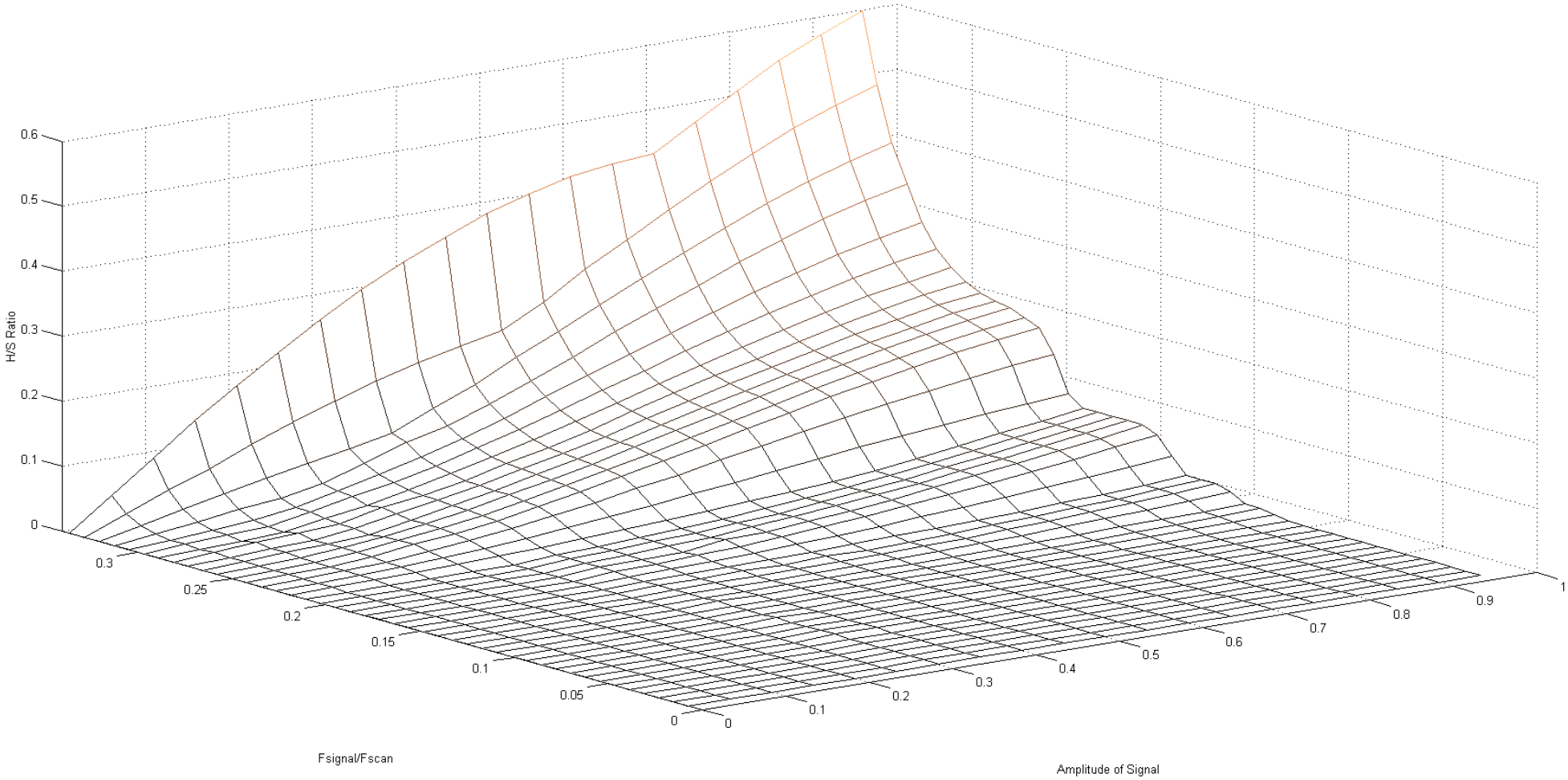

Figure 16. H/S ratio with 8th-order Butterworth type lowpass filter with $F_{cutoff} = 0.3*F_{scan}$

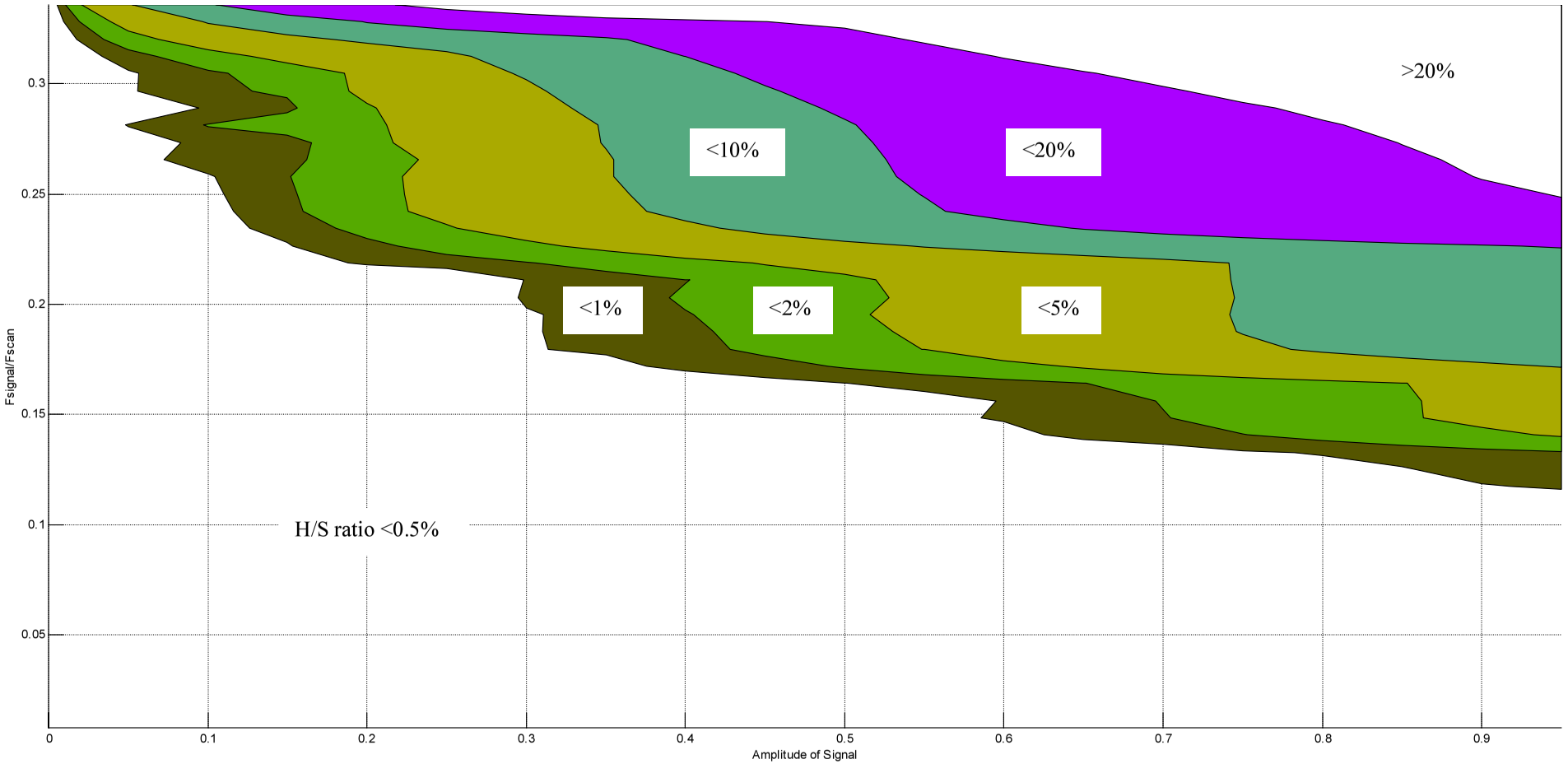

Figure 17. H/S ratio with 8th-order Butterworth type lowpass filter with $F_{cutoff} = 0.3*F_{scan}$